



Point-scale organic-matter decomposition in streambeds is weakly associated with reach-scale respiration

James C. Stegen^{1,2}, Morgan Barnes¹, Dillman Delgado¹, Brienne Forbes¹, Vanessa A. Garayburu-Caruso¹, Amy E. Goldman¹, Maggi Laan^{1,3}, Sophia McKeever¹, Peter Regier¹, Lupita Renteria¹, and Scott D. Tiegs⁴

¹Pacific Northwest National Laboratory, Richland, WA, United States

²Washington State University, Pullman, WA, United States

³University of California, Riverside, CA, United States

⁴Oakland University, Rochester, MI, United States

Correspondence: James C. Stegen (James.Stegen@pnl.gov)

Received: 6 December 2025 – Discussion started: 17 December 2025

Revised: 29 April 2026 – Accepted: 3 June 2026 – Published: 17 June 2026

Abstract. Stream and river ecosystems play a central role in the movement and decomposition of particulate organic matter, serving as a conduit between terrestrial hillslopes and coastal environments. Microbe-catalyzed decomposition generates simpler organic molecules that fuel respiration, often in the sediments of these ecosystems. However, the degree of connection between sediment-associated respiration (ER_{sed}) and organic-matter-decomposition potential remains poorly understood. It is also unclear whether organic-matter-decomposition potential is more closely associated with ER_{sed} , whole-ecosystem respiration (ER_{tot}), or water-column respiration (ER_{wc}). We examined the link between particulate organic-matter-decomposition potential – using cellulose-based cotton strips as a standardized substrate – and all three components of respiration across 48 sites in the environmentally diverse Yakima River Basin (Washington State, USA). We hypothesized that decomposition within sediments would be most strongly related to ER_{sed} , but decomposition rates were more closely associated with ER_{tot} , less so with ER_{sed} and not at all with ER_{wc} . This suggests that point-scale particulate organic-matter-decomposition potential within stream/river sediments is more closely associated with integrated system respiration rather than with processes confined to sediments or the water column alone though these relationships were weak overall. Further, across the basin, decomposition rates nearly spanned the previously reported global range for streams and rivers and were best explained by total dissolved nitrogen (TDN), sediment grain size, and aridity of the upstream drainage area. These results

highlight the strong influence of land cover and basin-scale biophysical variation on sediment-associated decomposition processes and indicate that mechanistic models of organic-matter decomposition in streams and rivers should account for coupled sediment–water–land interactions.

1 Introduction

Stream networks are major components of the global carbon cycle (Cole et al., 2007; Drake et al., 2018; Talluto et al., 2024). Whole-stream metabolism is often studied as an integrated outcome of processes occurring across the continuum from the air–water interface down through sediments that are below the stream itself (Battin et al., 2023; Tank et al., 2010). The sediments include the interface between the streambed and water column (i.e., the benthic zone) and the spatial domain below this interface, referred to as the hyporheic zone (Boulton et al., 1998; Krause et al., 2011; Wondzell, 2011). The benthic zone can be highly productive with significant primary producer (e.g., algae) and heterotrophic microbial biomass (Allan et al., 2021). The hyporheic zone is also highly biogeochemically active due, in part, to surface water flowing through it and mixing with groundwater to stimulate heterotrophic microbial activity (Boano et al., 2014; Lewandowski et al., 2019; Zarnetske et al., 2011). Processes occurring on and around sediments across the benthic-to-hyporheic continuum are often jointly responsible for the bulk of biogeochemical activity in stream systems (Burrows

et al., 2017; Fellows et al., 2001; Garayburu-Caruso et al., 2025; Naegeli and Uehlinger, 1997), with important exceptions in large rivers (Roley et al., 2023).

Metabolic processes within integrated stream systems are linked to the building of and breaking down of organic matter (Hall and Hotchkiss, 2017a; Odum, 1956). Streams are commonly net heterotrophic, meaning they mineralize more organic-matter-associated carbon than they fix by in-stream primary production (Battin et al., 2023; Bernhardt et al., 2022). This emphasizes the importance of understanding organic-matter decomposition in streams and its connection to respiration rates, which are ultimately linked to rates of elemental cycling. Organic-matter decomposition is commonly measured in stream systems by quantifying the breakdown of specific substrates (Benfield et al., 2017; Woodward et al., 2012). Cellulose-based cotton strips are an increasingly common model substrate for such studies as they enable broad comparisons across streams (and other types of ecosystems) (Colas et al., 2019; Filbee-Dexter et al., 2022; Tiegs et al., 2024; Vyšná et al., 2014). Like other standardized substrates used in decomposition studies (e.g., litter bags), cotton-strips quantify organic-matter-decomposition potential, that is, the capacity of the ecosystem to decompose organic matter, rather than the actual rate of native organic-matter decomposition in situ. A standard approach is to place them in the field for a known amount of time, retrieve them, and measure the loss in tensile strength, as a measure of the degree of decomposition. This approach has revealed many factors that impact decomposition in streams such as temperature, land use, aqueous chemistry, sediment texture, stream flow, location within the stream network, and canopy cover, among others (Griffiths and Tiegs, 2016; Tiegs et al., 2024).

Studies have examined the relationship between organic-matter decomposition and whole-stream respiration (Manusco et al., 2023; Pingram et al., 2020; Young and Collier, 2009), but have not specifically tied organic-matter decomposition within sediments to sediment-associated respiration. This leads to an open question and the focus of our study: To what degree are point-scale rates of organic-matter-decomposition potential within sediments linked to reach-scale respiration associated with the whole-stream ecosystem (ER_{tot}), the sediments (ER_{sed}), or the water column (ER_{wc})? ER_{tot} represents reach-scale aerobic respiration from autotrophs and heterotrophs across benthic, planktonic, and hyporheic zones. ER_{sed} comprises reach-scale sediment-associated respiration from benthic and streambed sediments, rooted and submerged plants, and hyporheic zones that are hydrologically connected to the active channel; ER_{wc} constitutes reach-scale planktonic respiration occurring only in the water column.

We specifically tested the hypothesis that reach-scale ER_{sed} rates are strongly linked to point-scale measurements of organic-matter decomposition within streambed sediments. More specifically, we tested the prediction that cotton-strip-decay rates are best explained by ER_{sed} , with little ad-

ditional variation in decay rates explained by ER_{tot} or ER_{wc} . To test our hypothesis and associated prediction we used field deployments across the Yakima River Basin (YRB). The YRB is an environmentally diverse basin in southeastern Washington State (USA) that is $\sim 16\,000\text{ km}^2$ and with a stream network that culminates in the 7th-order Yakima River. To generate the data needed to test our hypothesis, we used a combination of sensors and cotton strips across 48 sites in the YRB that collectively spanned a continuum from small mountainous streams in coniferous forests with little human impact to a large lowland river in an arid environment surrounded by significant agricultural land use. The resulting patterns help to fill a fundamental knowledge gap in our understanding of how point-scale organic-matter-decomposition potential relates to reach-scale respiration and can be used to inform models that aim to mechanistically integrate biogeochemical processes within and across stream networks.

2 Methods

To evaluate the linkages between organic-matter decomposition and stream ecosystem respiration we took advantage of a prior study (Garayburu-Caruso et al., 2025) that separated ER_{tot} , ER_{sed} , and ER_{wc} across environmentally divergent locations in the YRB (Fig. 1). Garayburu-Caruso et al. (2025) used dissolved oxygen (DO) sensors, dark bottle incubations, and the single-station method (Odum, 1956) to estimate these three components of respiration. In addition, that study deployed sensors to log water temperature, used here to calculate cumulative degree days as described below. These and associated contextual data were downloaded from existing data packages (Delgado et al., 2023; Forbes et al., 2023; Garayburu-Caruso et al., 2023), and methods are described in detail by Garayburu-Caruso et al. (2025). Data and computer scripts used in the current study are consolidated in Stegen et al. (2025). In brief, DO timeseries were analyzed via StreamMetabolizer (Appling et al., 2018) to estimate ER_{tot} . The length of the reach that a given DO sensor integrates varies across streams and has been estimated to be roughly three times the turnover length of O_2 (Hall and Hotchkiss, 2017b). As such, integrated reach lengths likely varied across sites due to differences in reaeration and discharge. Field sites were located in separate, non-overlapping reaches, helping to minimize potential spatial autocorrelation between neighboring sites in the estimated metabolic rates. To estimate ER_{wc} , 2 L opaque bottles containing a DO sensor were filled with stream water and incubated in situ; the rate of DO drawdown was used as the estimate of ER_{wc} . The difference between ER_{tot} and ER_{wc} was used as an estimate of ER_{sed} , which represents all respiration in the stream system that is not directly occurring in the water column. ER_{sed} therefore includes respiration in the hyporheic zone, the streambed surface, and rooted/submerged plants.

We note, however, that ER estimates derived from open diel O₂ methods capture all oxygen-consuming processes, not solely aerobic respiration. These estimates could also include abiotic oxidation of dissolved Fe(II) or the oxidation of other end products from anaerobic metabolism (Demars et al., 2015; Piatka et al., 2021), other oxidation processes such as nitrification and photooxidation of organic matter (Demars et al., 2015; Estapa and Mayer, 2010), or O₂ inputs from groundwater (Hall and Tank, 2005). Because ER_{sed} was calculated by the difference between ER_{tot} and ER_{wc}, it may be sensitive to these non-respiratory O₂ sinks. However, biological metabolism is generally considered the dominant O₂-consuming pathway in streams and we therefore interpret ER_{sed} primarily as sediment-associated biological O₂ consumption while acknowledging that other contributions may be captured.

To take advantage of the ecosystem respiration study, cotton strips made of Artist fabric (following the protocol of Tiegs et al., 2013) were deployed at the same time as the DO sensors. They were deployed upstream of the DO sensors to capture the upstream reach that influenced the DO sensor readings and prevent disturbance during sensor maintenance. This design prioritized among-reach coverage across the basin (48 sites) and provided point-scale estimates of decomposition potential at a single location within each reach.

The cotton strips were deployed in the shallow hyporheic zone for 35 continuous days at 48 sites across the YRB (Fig. 1). At each site, deployment locations were selected to be representative of the reach in terms of sediment size, flow velocity, and substrate composition. In larger river systems (e.g., 7th-order reaches), deployments were limited to wadeable areas near channel margins. Deployment and retrieval days varied across four days, but all strips were deployed for 35 d: deployments were from 25–28 July 2022 and retrievals were from 29 August–1 September 2022. Cotton strips were cut from bolts of 12-ounce, heavy-weight cotton fabric composed of 95 % cellulose (Style 548; Fredrix, Lawrenceville, GA, USA). Each strip was 27 threads wide and cut to 8.0 cm by 2.5 cm (after Tiegs et al., 2013). Each cotton strip was laid flat in a stainless-steel mesh cage (10.8 cm × 4.5 cm, RSV Jumbo Mesh Herb Infuser) to minimize physical damage and feeding by macroinvertebrates, thereby emphasizing microbe-based decomposition. At each site, four cages with one strip each were attached to the underside of clay bricks (20 cm × 10 cm × 5.5 cm) with stainless steel wire. The brick/cage/strip setup was nestled into streambed sediment such that the cages/strips were within the sediments and the brick was at the sediment/water interface. The four cages were next to each other. This setup kept the cotton strips out of direct light and within the sediments while allowing water to flow past the cotton strips.

After the 35 d incubation period, cotton strips were carefully removed from cages and gently brushed with gloved hands in stream water for approximately 10 s to remove large debris. Cleaned cotton strips were placed in 50 mL conical

centrifuge tubes with 70 % ethanol. Tubes were capped and rolled approximately 10 times before ethanol was removed. After completing this step, clean 70 % ethanol was added to the 50 mL tube to minimize further microbial-based decomposition. Cotton strips were transported in the ethanol filled tubes on blue ice to Pacific Northwest National Laboratory in Richland, WA. At the laboratory, the ethanol was removed from the tubes and cotton strips were air dried overnight prior to further drying in an oven at 40 °C for at least 24 h. After drying, cotton strips were stored in air-tight containers with desiccant.

Dried cotton strips were shipped to Oakland University, Rochester, MI for tensile-strength analysis following the protocol in Tiegs et al. (2013). A tensiometer was used to estimate tensile strength (Mark 10 MG100 with a Chatillon TCM 201 with roller jaws). The tensiometer pulled each cotton strip at a rate of 2 cm min⁻¹. Some of the cotton strips were completely degraded such that there was no material to measure, while other cages only contained fragments that were too small to measure tensile strength. These non-detect strips accounted for 5.4 % of all deployed strips. In both cases, a limit of detection was assigned as the lowest tensile strength calculated in Tiegs et al. (2019) divided by 2, resulting in a final value of 0.05. This was done to avoid statistical artifacts that can arise when simply introducing a value of 0 (i.e., the natural log transformation in Eq. 1 would be undefined). Removing these strips entirely would bias the analyses away from conditions with very fast decomposition.

Tensiometer data were converted into decay rates using tensile loss calculated via Eq. (1) (as in Mancuso et al., 2022).

$$K = \frac{-\ln(T_s/T_{sc})}{\text{Time}} \quad (1)$$

Here, K is the decomposition rate, T_s is the post-incubation tensile strength of the deployed cotton strips, and T_{sc} is the mean tensile strength of control strips that were not incubated in the field. The time variable was calculated as either the number of chronological deployment days (i.e., 35 d) or the number of degree days. Using degree days as the time variable accounts for variation in temperature across field sites and was estimated separately for each site as the sum of mean daily river temperature over the incubation period. We use K_{cd} and K_{dd} to represent decay rate per chronological day or per degree day, respectively. The values of K_{cd} and K_{dd} were estimated for each individual cotton strip and then replicates were averaged to provide a single site-level value for K_{cd} and K_{dd} .

We examined both K_{cd} and K_{dd} to evaluate whether the connection between decomposition and reach-scale respiration rates depends on accounting for temperature variation across the study basin. This is particularly relevant in the YRB because our field sites ranged from colder headwater streams to warmer low-gradient rivers. To test our hypothesis, we conducted both univariate and multivariate

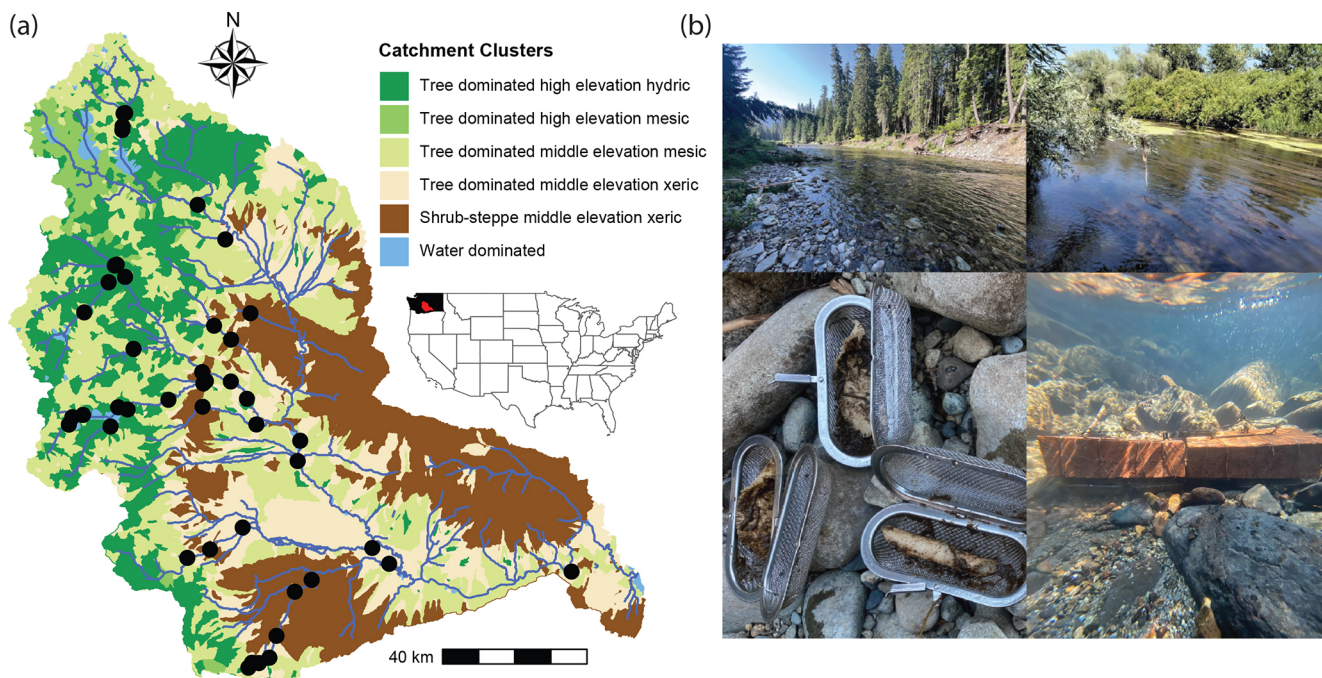


Figure 1. Biophysical clusters, sampling locations, and example conditions across the YRB. **(a)** The inset map shows the location of the YRB within the contiguous United States, with black indicating Washington State and red indicating the YRB. The YRB is shown with multiple colors, which correspond to biophysical clusters, as presented in Laan et al. (2025) and summarized briefly in the legend. Black circles are locations where decay rates were estimated. **(b)** Photos provide examples of the breadth of conditions studied across the YRB, post-incubation states of cotton strips, and deployment of the cotton strips.

regression-based analyses. We used ordinary least squares regression to examine the strength of univariate correlations between K_{cd} or K_{dd} and ER_{tot} , ER_{wc} , or ER_{sed} . We complemented this univariate analysis with multiple regression analysis to find an optimized model to explain variation in either K_{cd} or K_{dd} .

Further, to explore how other system variables may explain variation in decomposition rates, a LASSO (Least Absolute Shrinkage and Selection Operator) regression model was built using physical, chemical and environmental variables (Table S1 in the Supplement) as inputs, and K_{cd} or K_{dd} as the response variables. Variables were cube-root transformed and z -score normalized to reduce the impact of high leverage points in the regression analysis and to equally weight all variables. The LASSO regression was performed over 100 iterations, each with a different random seed using the `cv.glmnet` function in the `glmnet` R package (Friedman et al., 2010). β coefficients were normalized to the maximum β coefficient for each iteration, then averaged over the 100 iterations for the final reported value. Both the raw and normalized mean β coefficient and standard deviation are reported in addition to the R^2 (Table 2).

3 Results and Discussion

3.1 Decomposition in the Yakima River Basin spans globally reported rates

Both K_{cd} and K_{dd} exhibited a wide range of values (Fig. 2), effectively spanning the theoretical maximum of what could have been observed with our deployment setup. This is evidenced by some cotton strips being completely consumed prior to retrieval (5.4 % of all strips, K_{cd} and K_{dd} maximized), while others were largely intact (K_{cd} and $K_{dd} \approx 0$). This variation is surprising given the relatively small spatial domain sampled by this study, and emphasizes that environmental heterogeneity can surpass the effects of spatial extent (Mancuso et al., 2022). The environments studied here ranged from pristine locations in the mountainous headwaters of the YRB to lowland locations with heavy agricultural influences (Fig. 1; Laan et al., 2025). This emphasizes the value of environmentally diverse watersheds like the YRB as useful testbeds to study variation in decomposition rates within single hydrologically connected basins.

Comparing decay rates from the YRB to a global dataset from > 500 streams and rivers (Tiegs et al., 2024) showed that YRB rates spanned nearly the entire global range and had substantial overlap with the bulk of the global distributions (Fig. 2a and b). Dominant peaks in the YRB rate distri-

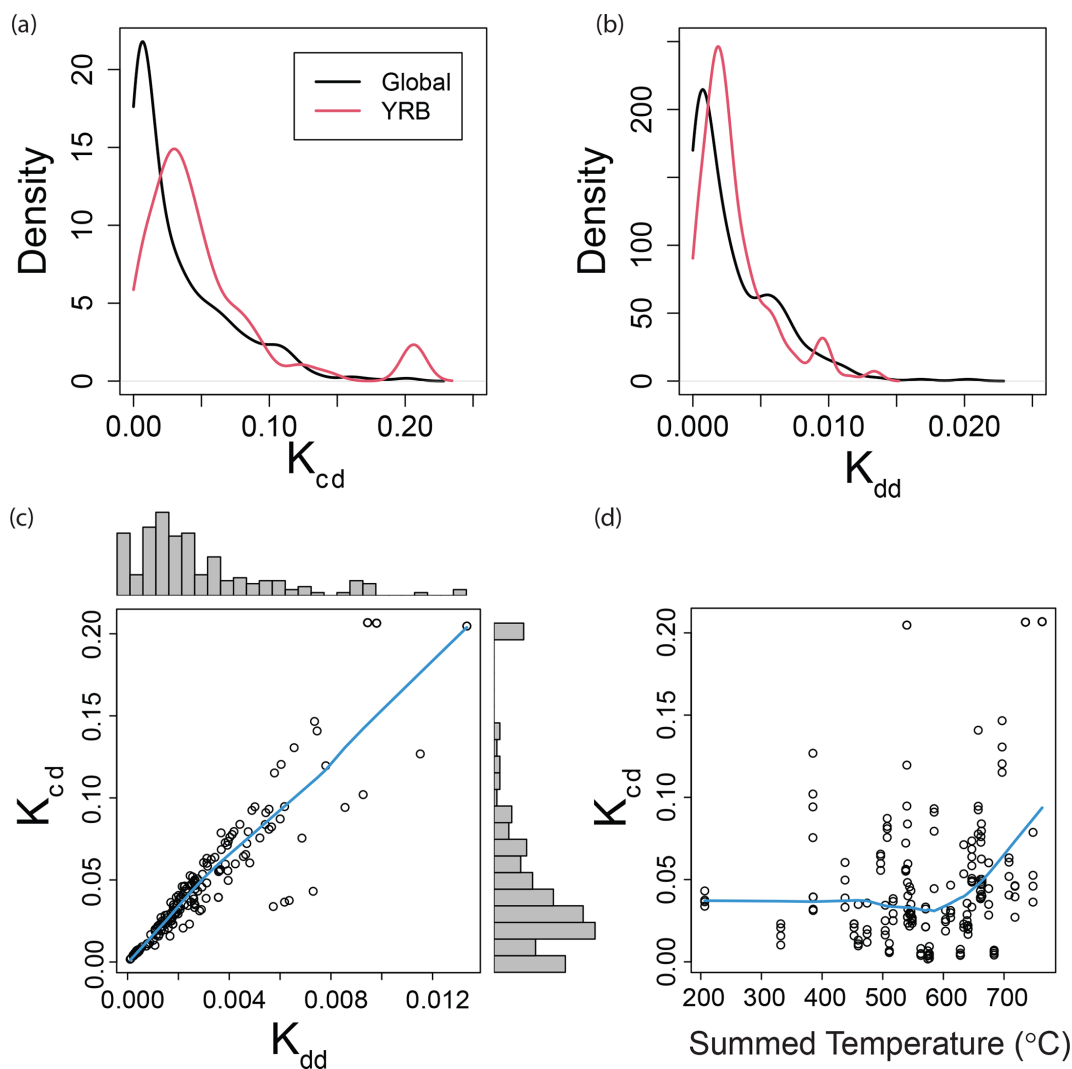


Figure 2. Decay rate distributions and relationships to each other and temperature. Kernel density functions for (a) K_{cd} and (b) K_{dd} from a global streams and rivers dataset and from the YRB. (c) Scatterplot correlating K_{cd} to K_{dd} . Histograms summarizing the distribution of each rate are provided on the outer boundaries. (d) K_{cd} related to temperature summed across the deployment period; summed temperature was used to calculate K_{dd} . Blue lines represent Lowess spline fits as regression analysis was not required for interpretation.

butions were shifted slightly towards faster rates, relative to primary peaks in the global dataset (Fig. 2a and b). This shift towards faster rates and the wide range in rates are likely due to several factors linked to rates being estimated in later summer with high temperatures, and established biological communities due to several months since high-flow disturbances (Collier et al., 2013b; Grimm and Fisher, 1989; Mancuso et al., 2023). The two decay rates were also closely correlated with each other, though the relationship weakened towards locations with faster decay rates (Fig. 2c). This suggests a weak influence of temperature in the YRB; a strong influence of temperature should lead to a weak relationship between K_{cd} and K_{dd} . These results contrast previously reported influences of temperature on particulate organic-matter decomposition (Benbi et al., 2014; Griffiths and Tiegs, 2016), and

likely reflect dominance of other influential factors such as variation in nutrient concentrations (Rosemond et al., 2015). Temperature-driven decomposition is also expected to lead to a strong relationship between K_{cd} and summed temperature, but we observed a very weak relationship despite ~ 4 -fold variation in summed temperature (Fig. 2d). This range in temperature among sites would likely be smaller in other seasons, and we do not therefore expect a strong influence of temperature to emerge in the YRB by conducting the study in other seasons. These results emphasize the need to understand factors governing variation in decay rates across the YRB. This is especially true given that rate distributions within this one basin span nearly all globally observed decay rates.

Across the YRB there appears to be potential for some spatial organization for both K_{cd} and K_{dd} (Fig. 3). Visual inspection of the maps suggests that the spatial organization may be stronger for K_{cd} than for K_{dd} . To evaluate this possibility more rigorously, we regressed each decay rate against upstream drainage area (Fig. 4). In this case, drainage area is meant to reflect position within the YRB. We used drainage area in preference to stream order because it is a continuous variable directly tied to the spatial domain a given stream integrates, whereas stream order is categorical and primarily reflects stream network topology. Associated regressions were significant ($p < 0.05$) with both decay rates increasing with drainage area (Fig. 4). The relationship with drainage area was stronger, in terms of R^2 , for K_{cd} . Both relationships were, however, relatively weak with R^2 values of 0.22 and 0.14 for K_{cd} and K_{dd} , respectively (Fig. 4). Nonetheless, the existence of a significant relationship after controlling for temperature (i.e., for K_{dd}) indicates that spatially structured factors other than temperature influence decay rates. This is not surprising as studies using cotton strips have found several factors that influence decomposition, such as nutrient concentrations, turbidity, and many others (Collier et al., 2013b; Pingram et al., 2020; Tiegs et al., 2024). Before exploring a broad suite of potential explanatory variables, we tested our hypothesis that decomposition rates will be better explained by sediment-associated respiration (ER_{sed}) than by respiration in the water column (ER_{wc}) or by respiration of the integrated stream system (ER_{tot}).

3.2 Respiration in sediments explains little variation in decomposition

Contrary to our hypothesis, we found that both decay rates were most strongly connected to ER_{tot} , less so with ER_{sed} , and not at all with ER_{wc} (Fig. 5). Univariate models using ER_{tot} were better than multivariate models using ER_{sed} , ER_{wc} , and their interaction. This is evidenced by univariate models using ER_{tot} having AIC values more than two units lower than multivariate models containing ER_{sed} and ER_{wc} (Table 1). Multivariate models were not used with ER_{tot} because it contains ER_{sed} and ER_{wc} . Garayburu-Caruso et al. (2025) showed that ER_{sed} accounted for the majority of ER_{tot} across most of the YRB, with 88 % of locations showing ER_{sed} contributions exceeding 50 % of ER_{tot} . The strong correspondence between these two metrics might explain the similar R^2 values observed. We note, however, that the difference in explained variance between ER_{tot} ($R^2 = 0.29$ for K_{cd} ; $R^2 = 0.16$ for K_{dd}) and ER_{sed} ($R^2 = 0.22$ for K_{cd} ; $R^2 = 0.13$ for K_{dd}) was modest, and the stronger association with ER_{tot} should be interpreted cautiously.

To interpret these results, we note that cotton strips were deployed a few centimeters into the riverbed sediments, beneath a brick set flush with the streambed surface. We conceptualized this deployment as the shallow hyporheic zone, which was a reason we hypothesized that decay rates would

Table 1. Comparison of univariate and multivariate regression models explaining variation in K_{cd} and K_{dd} . Model structures are indicated, along with change in AIC relative to the best model. ER_{tot} was not used in multivariate models because $ER_{tot} = ER_{sed} + ER_{wc}$. Regression statistics for the univariate models are provided in Fig. 5; only the best performing univariate models, in terms of R^2 , are shown. The models with ER_{sed} and ER_{wc} , but not the interaction term, are effectively the same as the ER_{tot} model because $ER_{tot} = ER_{sed} + ER_{wc}$. They are included as a point of reference for the model that also includes the $ER_{sed} \times ER_{wc}$ interaction term.

Model	Δ AIC
$K_{cd} \sim ER_{tot}$	0
$K_{cd} \sim ER_{sed} + ER_{wc}$	3.8
$K_{cd} \sim ER_{sed} + ER_{wc} + ER_{sed} \times ER_{wc}$	5.7
$K_{dd} \sim ER_{tot}$	0
$K_{dd} \sim ER_{sed} + ER_{wc}$	3.0
$K_{dd} \sim ER_{sed} + ER_{wc} + ER_{sed} \times ER_{wc}$	4.8

be most strongly connected to ER_{sed} . However, the results indicate that point-scale decomposition of particulate organic matter within the shallow hyporheic zone is linked to respiratory processes occurring in both the sediment and water column. Therefore, our deployment depth might have reflected sediment-water interface processes in addition to shallow hyporheic zone processes, leading to stronger associations of cotton strip decomposition with ER_{tot} . We also note that ER_{sed} estimates may not exclusively reflect biological respiration, as non-respiratory O_2 -consuming processes can contribute to these estimates (see Methods). We propose that if our deployment configuration was complemented with a simultaneous deployment that enabled growth of benthic algal biofilms on the cotton strips, the combined decomposition from both deployments could, in some systems, capture more of the processes that contribute to ER_{sed} . This would provide a more complete view of sediment-associated biogeochemical function, potentially leading to a stronger correlation between decomposition rates and ER_{sed} . While this remains to be tested, the underlying idea is that primary producers support a large portion of respiration associated with riverbed sediments, which is supported by recent analyses showing a strong link between ER_{sed} and gross primary production across the YRB (Garayburu-Caruso et al., 2025).

3.3 Slower rates of K_{cd} and K_{dd} are in streams with coarse sediments, set within wet forests

Given that our hypothesis was rejected and that ER_{tot} explained only about 29 % and 16 % of K_{cd} and K_{dd} , respectively (Table 1 and Fig. 5), we used a discovery-based approach to explore other system variables that may explain further variation in decomposition rates. LASSO-based modeling indicated that total dissolved nitrogen (TDN) and the median grain size of sediment texture (D50) were most im-

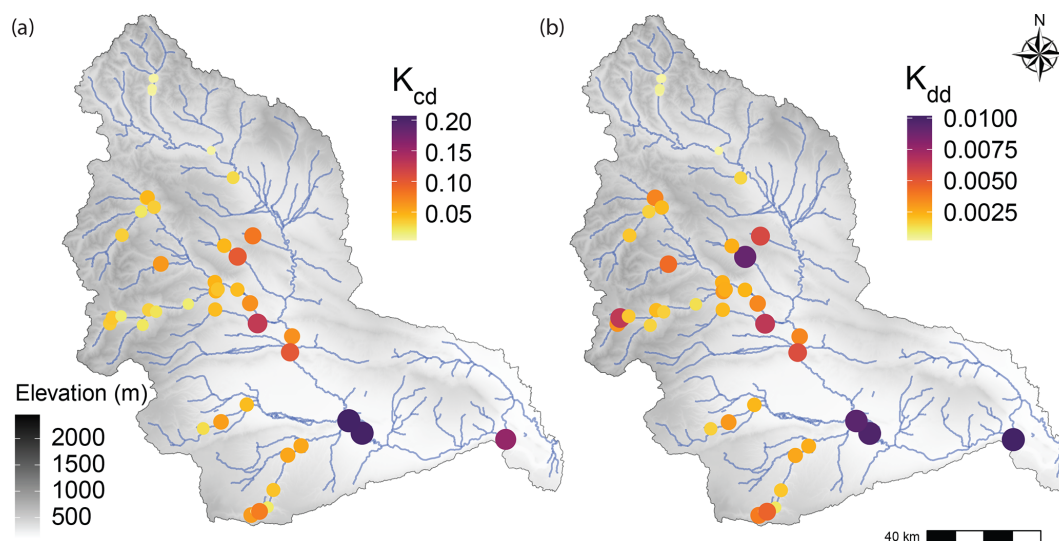


Figure 3. Spatial distribution of decay rates across the YRB. Each map shows elevation profiles and either K_{cd} (a) or K_{dd} (b). Colored circles are field locations where rates were estimated. The color of each circle is related to decay rate as indicated in the legends, and circle size is scaled to decay rate to further facilitate visual interpretability.

portant for explaining K_{dd} , while TDN and aridity were most important for explaining K_{cd} (Table 2). Other variables were retained in the LASSO models (Table S1), but we interpreted TDN, D50, and aridity as the most important because they consistently had the largest normalized coefficients. This interpretation is based on these variables having mean normalized coefficients above 0.5 – in terms of absolute value – meaning they were at least 50 % as important as the most important variable in the 100 LASSO model runs. Further, the LASSO coefficients for these variables had a coefficient of variation less than 0.5, meaning that across the 100 LASSO model runs the values of their normalized coefficients were relatively stable (Table S1). The LASSO modeling also confirmed a relatively weak influence of temperature, evidenced by relatively small and highly variable β coefficients for summed temperature in the K_{cd} model (Table S1); temperature was not used in the K_{dd} model.

Both decomposition rates increased with higher TDN concentrations, while K_{dd} decreased with larger D50 and K_{cd} decreased with higher aridity index values (Table 2). To more deeply interpret these relationships, we examined Pearson-based univariate correlations between these three explanatory variables and other variables included in the LASSO models. This is important because of strong collinearity among some explanatory variables (Fig. S1 in the Supplement). In this case, variables identified as being the most important may be acting as proxies for one or more additional variables. We found that TDN was most strongly correlated with percent agricultural land cover of the upstream drainage area and sulfate concentrations in the stream water (Fig. S1). Increases in both decomposition rates with TDN may, therefore, reflect agricultural inputs of nutrients that increase overall mi-

crobial activity of the stream ecosystems we studied. D50 was most strongly correlated with the aridity index, which was most strongly correlated with percent forest cover; the correlation between D50 and aridity is unlikely to reflect a causal connection, while aridity and forest cover most likely are causally linked. If the relationship between decomposition and D50 is causal, it could be mediated by the total surface area available for microbial attachment. This would, however, influence decomposition only to the extent that microbial biomass in adjacent sediments impacts microbial activity on the cotton strips. Coarser sediments have much less surface area, potentially limiting overall microbial activity.

Considering the directionality of the univariate relationships, in context of the LASSO outcomes, suggests slower decomposition – for both rates – in streams with relatively coarse sediments and set within relatively wet forests. This contrasts with Clapcott and Barnuta (2010) who found faster decomposition in coarser sediments. The discrepancy is likely because we excluded macroinvertebrates while they did not, and they interpreted the link to sediment texture as due to greater habitat availability for macroinvertebrates in coarser sediments. Locations with slower decomposition should, thus, primarily be in higher elevation, relatively pristine parts of the YRB, while faster decomposition occurs at lower elevations impacted by agricultural inputs. These results are consistent with previous work showing greater cotton strip decomposition in impaired streams (Young and Collier, 2009), those with little natural land cover (Collier et al., 2013a; Webb et al., 2019), and in streams with higher nutrient concentrations (Ferreira et al., 2015; Pingram et al., 2020; Tiegs et al., 2013). In addition to differences in nutrient concentrations between higher and lower elevation sites, we ex-

Table 2. Regression coefficients from LASSO models explaining variation in K_{dd} and K_{cd} . Explanatory variables were cube-root transformed to reduce influence from high leverage data points and standardized as z-scores to enable direct comparison of the regression coefficients. LASSO models were fit over 100 seeds. Regression coefficients (β) and R^2 values were averaged across the 100 seeds. Normalized regression coefficients were calculated by dividing each β coefficient by the maximum β coefficient in each seed. Standard deviation (sd) is reported for each variables' coefficient over the 100 seeds and used to calculate the coefficient of variation (cv). Variables shown have an absolute value of mean normalized β of > 0.5 and $cv < 0.5$ to emphasize variables that were consistently important across seeds. Results for all variables, both normalized and not normalized, can be found in Table S1.

Response Variable	Predictor Variable	Mean Normalized Regression Coefficient (β)	sd	cv
K_{dd}	Water TDN	1	0	0
	D50	-0.699	0.087	-0.124
Mean R^2		0.502 (sd = 0.0673)		
K_{cd}	Aridity	-0.959	0.065	-0.067
	Water TDN	0.805	0.156	0.193
Mean R^2		0.883 (sd = 0.083)		

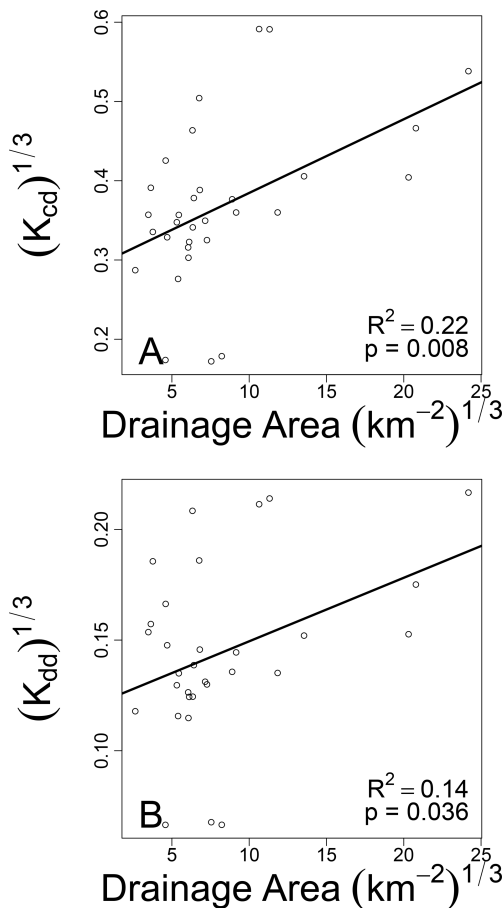


Figure 4. Decay rates increase with drainage area. K_{cd} (A) and K_{dd} (B) regressed against upstream drainage area and fit with an ordinary least squares linear regression. Associated regression models are shown as solid black lines and statistics are provided on each panel. Data were cube-root transformed to improve normality before analysis.

pect less light penetration to streams in higher elevation sites because of more forest cover and smaller streams. Though not measured here, less light could suppress autotrophic production which may limit heterotrophic respiration (Bernhardt et al., 2022; Mulholland et al., 2001; Young and Huryn, 1999). Lower autotrophic production could therefore slow decomposition relative to high-light conditions by reducing the supply of labile carbon from phototrophs that can prime organic-matter degradation (Danger et al., 2013; Howard-Parker et al., 2020).

3.4 Point-scale decomposition is associated with processes across the sediment-water continuum and land features

Our results collectively indicate that to study shallow hyporheic zone decomposition processes, it is not sufficient to conceptualize organic-matter decomposition by only considering sediment or water column processes; one must examine the integrated system. The implication of our analyses is that point-scale organic-matter decomposition potential was more closely associated with integrated system respiration than with individual respiration components. Our findings suggest that mechanistic models of stream ecosystem respiration may benefit from accounting for sediment processes, water-column processes, and land-cover influences from beyond the stream. Focusing exclusively on the hyporheic zone is insufficient, even in systems for which the hyporheic zone accounts for most reactions (Boano et al., 2014; Burrows et al., 2017; McClain et al., 2003). This is further emphasized by previous work showing that most respiration occurs in the water column of large rivers (Gardner and Doyle, 2018; Roley et al., 2023). Garayburu-Caruso et al. (2025) also show that fractional contributions of ER_{sed} to ER_{tot} is often high, but that there is significant variation in those fractional influences across the YRB. This variability is due to ER_{wc} being fast enough, in some locations, to ac-

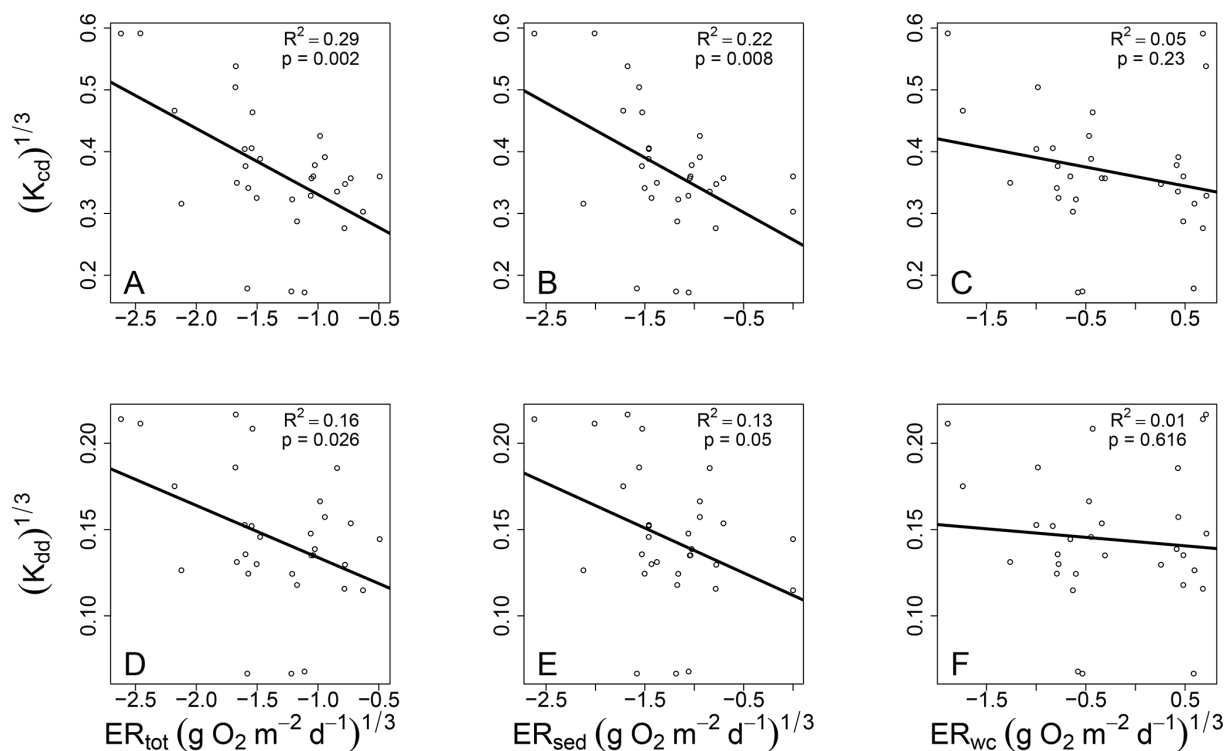


Figure 5. Decay rates related to each of the three aspects of stream ecosystem respiration. Both K_{cd} (A–C) and K_{dd} (D–F) show strongest relationships with ER_{tot} (A, D), weaker relationships with ER_{sed} (B, E), and non-significant relationships with ER_{wc} (C, F). Ordinary least squares linear regression models are shown with solid black lines and associated statistics are provided on each panel. All variables were cube-root transformed to improve normality prior to regression analysis.

count for more than 80 % of ER_{tot} (Garayburu-Caruso et al., 2025). Similarly, Laan et al. (2025) found substantial overlap between the distribution of ER_{wc} rates from the YRB and ER_{tot} from across the contiguous United States. The overall picture is that decomposition is the result of integrated processes occurring across the sediment-water continuum and influenced by external factors tied to land cover and land use. We infer that these integrated processes are influenced by biophysical variation across the YRB (Laan et al., 2025), leading to decomposition rates within this single basin that resemble global rate distributions and nearly span the global range of observed rates (Tiegs et al., 2024). Other basins that contain only one ecoregion or have homogeneous land cover may be expected to have a narrower range of decomposition rates (Webb et al., 2019). We note that our decomposition estimates represent point-scale conditions at wadeable locations and should be interpreted as such rather than as reach-integrated measures of decomposition. Capturing within-reach spatial variability in decomposition across habitats and channel depths would complement the among-reach approach used here, and may lead to stronger relationships between decomposition rates and reach-scale ER. Nonetheless, models applied to any stream network that aim to predict spatiotemporal variation in decomposition rates would

be well served by considering processes throughout the integrated watershed system.

Code and data availability. Data and scripts used to generate the main findings within this manuscript can be found at <https://data.ess-dive.lbl.gov/view/doi:10.15485/3008446>, last access: 12 June 2025 (Stegen et al., 2025). Other data collected during the field efforts (i.e., raw sensor data, surface water chemistry data, geospatial and environmental metadata, and respiration rates for the 2022 Spatial Study sampling event) can be accessed on ESS-DIVE at <https://data.ess-dive.lbl.gov/datasets/doi:10.15485/1987520>, last access: 12 June 2025 (Garayburu-Caruso et al., 2023), <https://data.ess-dive.lbl.gov/datasets/doi:10.15485/1969566>, last access: 12 June 2025 (Delgado et al., 2023), and <https://data.ess-dive.lbl.gov/datasets/doi:10.15485/1923689>, last access: 12 June 2025 (Forbes et al., 2023).

Supplement. The supplement related to this article is available online at <https://doi.org/10.5194/bg-23-3981-2026-supplement>.

Author contributions. Conceptualization: JCS, MB, VAG-C, PR, SDT; Data Curation: MB, JCS, BF, ML, SM, DD, LR and AEG; Formal Analysis: MB, MML, BF, and JCS; Funding Acquisition:

JCS; Investigation: MB, DD, BF, VAG-C, AEG, ML, SM, PR, LR, SDT and JCS; Methodology: MB, DD, BF, VAG-C, AEG, ML, SM, PR, LR, SDT and JCS; Project Administration: MB, VAG-C and JCS; Resources: MB, DD, BF, VAG-C, AEG, ML, SM, PR, LR, SDT and JCS; Software: MB, MML, BF, and JCS; Supervision: MB, VAG-C and JCS; Validation: MB and JCS; Visualization: MB, MML, BF, and JCS; Writing – Original Draft Preparation: MB, VAG-C, SDT and JCS; Writing – Review and Editing: MB, DD, BF, VAG-C, AEG, ML, SM, PR, LR, SDT and JCS.

Competing interests. The contact author has declared that none of the authors has any competing interests.

Disclaimer. Publisher's note: Copernicus Publications remains neutral with regard to jurisdictional claims made in the text, published maps, institutional affiliations, or any other geographical representation in this paper. The authors bear the ultimate responsibility for providing appropriate place names. Views expressed in the text are those of the authors and do not necessarily reflect the views of the publisher.

Acknowledgements. This work was supported by the River Corridor Science Focus Area (RC-SFA) at the Pacific Northwest National Laboratory (PNNL). The RC-SFA is supported by the United States Department of Energy, Office of Biological and Environmental Research (BER), Environmental System Science (ESS) Program. PNNL is operated by Battelle Memorial Institute for the United States Department of Energy under contract no. DE-AC05-76RL01830. We thank the United States Forest Service, Washington Department of Natural Resources, Washington Department of Fish and Wildlife, Confederated Tribes and Bands of the Yakama Nation, and Cowiche Canyon Conservancy for access to field locations where these samples were collected. We also thank the Confederated Tribes and Bands of the Yakama Nation Tribal Council and Yakama Nation Fisheries for working with us to facilitate sample collection and optimization of data usage according to their values and worldview. We thank the field team including: Dillman Delgado, Morgan Barnes, Brandon T. Boehnke, Yunxiang Chen, Kali Cornwell, Brianna I. Gonzalez, Samantha Grieger, Glenn E. Hammond, Peishi Jiang, Bing Li, Zhi Li, Xinming Lin, Sophia A. McKeever, Maruti K. Mudunuru, Katherine A. Muller, Opal Otenburg, Aaron Pelly, Kelsey Peta, Alan Roebuck, Joshua M. Torgeson, and Jianqiu Zheng.

Financial support. This research has been supported by the U.S. Department of Energy, Office of Science (grant no. 54737).

Review statement. This paper was edited by Lishan Ran and reviewed by Arturo Elosegi and two anonymous referees.

References

- Allan, J. D., Castillo, M. M., and Capps, K. A.: Stream Ecology: Structure and Function of Running Waters, Springer International Publishing, Cham, <https://doi.org/10.1007/978-3-030-61286-3>, 2021.
- Appling, A. P., Hall Jr., R. O., Yackulic, C. B., and Arroita, M.: Overcoming Equifinality: Leveraging Long Time Series for Stream Metabolism Estimation, *J. Geophys. Res.-Biogeo.*, 123, 624–645, <https://doi.org/10.1002/2017JG004140>, 2018.
- Battin, T. J., Lauerwald, R., Bernhardt, E. S., Bertuzzo, E., Gener, L. G., Hall, R. O., Hotchkiss, E. R., Maavara, T., Pavelsky, T. M., Ran, L., Raymond, P., Rosentreter, J. A., and Regnier, P.: River ecosystem metabolism and carbon biogeochemistry in a changing world, *Nature*, 613, 449–459, <https://doi.org/10.1038/s41586-022-05500-8>, 2023.
- Benbi, D. K., Boparai, A. K., and Brar, K.: Decomposition of particulate organic matter is more sensitive to temperature than the mineral associated organic matter, *Soil Biol. Biochem.*, 70, 183–192, <https://doi.org/10.1016/j.soilbio.2013.12.032>, 2014.
- Benfield, E. F., Fritz, K. M., and Tiegs, S. D.: Leaf-Litter Breakdown, Chapt. 27, in: *Methods in Stream Ecology*, 3rd edn., edited by: Lamberti, G. A. and Hauer, F. R., Academic Press, 71–82, <https://doi.org/10.1016/B978-0-12-813047-6.00005-X>, 2017.
- Bernhardt, E. S., Savoy, P., Vlah, M. J., Appling, A. P., Koenig, L. E., Hall, R. O., Arroita, M., Blaszczyk, J. R., Carter, A. M., Cohen, M., Harvey, J. W., Heffernan, J. B., Helton, A. M., Hosen, J. D., Kirk, L., McDowell, W. H., Stanley, E. H., Yackulic, C. B., and Grimm, N. B.: Light and flow regimes regulate the metabolism of rivers, *P. Natl. Acad. Sci. USA*, 119, e2121976119, <https://doi.org/10.1073/pnas.2121976119>, 2022.
- Boano, F., Harvey, J. W., Marion, A., Packman, A. I., Revelli, R., Ridolfi, L., and Wörman, A.: Hyporheic flow and transport processes: Mechanisms, models, and biogeochemical implications, *Rev. Geophys.*, 52, 603–679, <https://doi.org/10.1002/2012RG000417>, 2014.
- Boulton, A. J., Findlay, S., Marmonier, P., Stanley, E. H., and Valett, H. M.: The functional significance of the hyporheic zone in streams and rivers, *Annu. Rev. Ecol. Evol. S.*, 29, 59–81, <https://doi.org/10.1146/annurev.ecolsys.29.1.59>, 1998.
- Burrows, R. M., Rutledge, H., Bond, N. R., Eberhard, S. M., Auhl, A., Andersen, M. S., Valdez, D. G., and Kennard, M. J.: High rates of organic carbon processing in the hyporheic zone of intermittent streams, *Sci. Rep.-UK*, 7, 13198, <https://doi.org/10.1038/s41598-017-12957-5>, 2017.
- Clapcott, J. E. and Barmuta, L. A.: Metabolic patch dynamics in small headwater streams: exploring spatial and temporal variability in benthic processes, *Freshwater Biol.*, 55, 806–824, <https://doi.org/10.1111/j.1365-2427.2009.02324.x>, 2010.
- Colas, F., Woodward, G., Burdon, F. J., Guérol, F., Chauvet, E., Cornut, J., Cébron, A., Clivot, H., Danger, M., Danner, M. C., Pagnout, C., and Tiegs, S. D.: Towards a simple global-standard bioassay for a key ecosystem process: organic-matter decomposition using cotton strips, *Ecol. Indic.*, 106, 105466, <https://doi.org/10.1016/j.ecolind.2019.105466>, 2019.
- Cole, J. J., Prairie, Y. T., Caraco, N. F., McDowell, W. H., Tranvik, L. J., Striegl, R. G., Duarte, C. M., Kortelainen, P., Downing, J. A., Middelburg, J. J., and Melack, J.: Plumbing the Global Carbon Cycle: Integrating Inland Waters into

- the Terrestrial Carbon Budget, *Ecosystems*, 10, 172–185, <https://doi.org/10.1007/s10021-006-9013-8>, 2007.
- Collier, K. J., Clapcott, J. E., Hamer, M. P., and Young, R. G.: Extent estimates and land cover relationships for functional indicators in non-wadeable rivers, *Ecol. Indic.*, 34, 53–59, <https://doi.org/10.1016/j.ecolind.2013.04.010>, 2013a.
- Collier, K. J., Clapcott, J. E., Duggan, I. C., Hamilton, D. P., Hamer, M., and Young, R. G.: Spatial Variation of Structural and Functional Indicators in a Large New Zealand River, *River Res. Appl.*, 29, 1277–1290, <https://doi.org/10.1002/rra.2609>, 2013b.
- Danger, M., Cornut, J., Chauvet, E., Chavez, P., Elger, A., and Lecerf, A.: Benthic algae stimulate leaf litter decomposition in detritus-based headwater streams: a case of aquatic priming effect?, *Ecology*, 94, 1604–1613, <https://doi.org/10.1890/12-0606.1>, 2013.
- Delgado, D., Barnes, M., Boehnke, B. T., Chen, X., Chen, Y., Cornwell, K., Forbes, B., Fulton, S. G., Garayburu-Caruso, V. A., Goldman, A. E., Gonzalez, B. I., Grieger, S., Hammond, G. E., Jiang, P., Kaufman, M. H., Laan, M., Li, B., Li, Z., Lin, X., McKeever, S. A., Mudunuru, M. K., Muller, K. A., Myers-Pigg, A., Otenburg, O., Pelly, A., Peta, K., Powers-McCormack, B., Regier, P., Renteria, L., Roebuck, A., Scheibe, T. D., Son, K., Torgeson, J. M., Zheng, J., and Stegen, J. C.: Spatial Study 2022: Surface Water Samples, Cotton Strip Degradation, and Hydrologic Sensor Data across the Yakima River Basin, Washington, USA (v3), River Corridor and Watershed Biogeochemistry SFA, ESS-DIVE repository [data set], <https://doi.org/10.15485/1969566>, 2023.
- Demars, B. O. L., Thompson, J., and Manson, J. R.: Stream metabolism and the open diel oxygen method: Principles, practice, and perspectives, *Limnol. Oceanogr.-Meth.*, 13, 356–374, <https://doi.org/10.1002/lom3.10030>, 2015.
- Drake, T. W., Raymond, P. A., and Spencer, R. G. M.: Terrestrial carbon inputs to inland waters: A current synthesis of estimates and uncertainty, *Limnology and Oceanography Letters*, 3, 132–142, <https://doi.org/10.1002/lo2.10055>, 2018.
- Estapa, M. L. and Mayer, L. M.: Photooxidation of particulate organic matter, carbon/oxygen stoichiometry, and related photoreactions, *Mar. Chem.*, 122, 138–147, <https://doi.org/10.1016/j.marchem.2010.06.003>, 2010.
- Fellows, C. S., Valett, M. H., and Dahm, C. N.: Whole stream metabolism in two montane streams: Contribution of the hyporheic zone, *Limnol. Oceanogr.*, 46, 523–531, <https://doi.org/10.4319/lo.2001.46.3.0523>, 2001.
- Ferreira, V., Castagnyrol, B., Koricheva, J., Gulis, V., Chauvet, E., and Graça, M. A. S.: A meta-analysis of the effects of nutrient enrichment on litter decomposition in streams, *Biol. Rev.*, 90, 669–688, <https://doi.org/10.1111/brv.12125>, 2015.
- Filbee-Dexter, K., Feehan, C. J., Smale, D. A., Krumhansl, K. A., Augustine, S., Bettignies, F. de, Burrows, M. T., Byrnes, J. E. K., Campbell, J., Davoult, D., Dunton, K. H., Franco, J. N., Garrido, I., Grace, S. P., Hancke, K., Johnson, L. E., Konar, B., Moore, P. J., Norderhaug, K. M., O'Dell, A., Pedersen, M. F., Salomon, A. K., Sousa-Pinto, I., Tiegs, S., Yiu, D., and Wernberg, T.: Kelp carbon sink potential decreases with warming due to accelerating decomposition, *PLOS Biol.*, 20, e3001702, <https://doi.org/10.1371/journal.pbio.3001702>, 2022.
- Forbes, B., Barnes, M., Boehnke, B. T., Bowden, M. E., Chen, X., Cornwell, K., Crawford, M., Delgado, D., Fulton, S. G., Garayburu-Caruso, V. A., Gary, S., Goldman, A. E., Gonzalez, B. I., Grieger, S., Hammond, G. E., Jiang, P., Kaufman, M. H., Laan, M., Li, B., Li, Z., McKeever, S. A., Mudunuru, M. K., Muller, K. A., Myers-Pigg, A., Otenburg, O., Pelly, A., Peta, K., Powers-McCormack, B., Regier, P., Renteria, L., Roebuck, A., Scheibe, T. D., Son, K., Tfaily, M. M., Torgeson, J. M., Stegen, J. C., and Consortium, T. W.: WHONDRS River Corridor Sediment and Water Geochemistry and In Situ Sensor Data from Machine-Learning-Informed Sites across the Contiguous United States (v6), River Corridor and Watershed Biogeochemistry SFA, ESS-DIVE Repository [data set], <https://doi.org/10.15485/1923689>, 2023.
- Friedman, J., Hastie, T., and Tibshirani, R.: Regularization Paths for Generalized Linear Models via Coordinate Descent, *J. Stat. Softw.*, 33, 1–22, <https://doi.org/10.18637/jss.v033.i01>, 2010.
- Garayburu-Caruso, V. A., Kaufman, M. H., Delgado, D., Barnes, M., Boehnke, B. T., Chen, X., Cornwell, K., Forbes, B., Fulton, S. G., Goldman, A. E., Gonzalez, B. I., Grieger, S., Jr, R. O. H., Hammond, G. E., Jiang, P., Laan, M., Li, B., Li, Z., Lin, X., McKeever, S. A., Mudunuru, M. K., Muller, K. A., Myers-Pigg, A., Otenburg, O., Pelly, A., Peta, K., Regier, P., Renteria, L., Roebuck, A., Scheibe, T. D., Son, K., Torgeson, J. M., and Stegen, J. C.: Spatial Study 2022: Water Column, Sediment, and Total Ecosystem Respiration Rates across the Yakima River Basin, Washington, USA (v2), River Corridor Hydro-biogeochemistry from Molecular to Multi-Basin Scales SFA, ESS-DIVE repository [data set], <https://doi.org/10.15485/1987520>, 2023.
- Garayburu-Caruso, V. A., Kaufman, M., Forbes, B., Hall, R. O., Laan, M., Chen, X., Lin, X., Fulton, S., Renteria, L., Fang, Y., Son, K., and Stegen, J. C.: Sediment-associated processes account for most of the spatial variation in ecosystem respiration in the Yakima River basin, *bioRxiv*, 2024.03.22.586339, <https://doi.org/10.1101/2024.03.22.586339>, 2025.
- Gardner, J. R. and Doyle, M. W.: Sediment–Water Surface Area Along Rivers: Water Column Versus Benthic, *Ecosystems*, 21, 1505–1520, <https://doi.org/10.1007/s10021-018-0236-2>, 2018.
- Griffiths, N. A. and Tiegs, S. D.: Organic-matter decomposition along a temperature gradient in a forested headwater stream, *Freshw. Sci.*, 35, 518–533, 2016.
- Grimm, N. B. and Fisher, S. G.: Stability of Periphyton and Macroinvertebrates to Disturbance by Flash Floods in a Desert Stream, *J. N. Am. Benthol. Soc.*, 8, 293–307, <https://doi.org/10.2307/1467493>, 1989.
- Hall, R. O. and Hotchkiss, E. R.: Chapter 34 - Stream Metabolism, in: *Methods in Stream Ecology*, 4rd edn., edited by: Lamberti, G. A. and Hauer, F. R., Academic Press, 219–233, <https://doi.org/10.1016/B978-0-12-813047-6.00012-7>, 2017a.
- Hall, R. O. and Hotchkiss, E. R.: Stream Metabolism, in: *Methods in Stream Ecology*, Academic Press, 219–233, <https://doi.org/10.1016/B978-0-12-813047-6.00012-7>, 2017b.
- Hall, R. O. and Tank, J. L.: Correcting whole-stream estimates of metabolism for groundwater input, *Limnol. Oceanogr.-Meth.*, 3, 222–229, <https://doi.org/10.4319/lom.2005.3.222>, 2005.
- Howard-Parker, B., White, B., Halvorson, H. M., and Evans-White, M. A.: Light and dissolved nutrients mediate recalcitrant organic matter decomposition via microbial priming

- in experimental streams, *Freshwater Biol.*, 65, 1189–1199, <https://doi.org/10.1111/fwb.13503>, 2020.
- Krause, S., Hannah, D. M., Fleckenstein, J. H., Heppell, C. M., Kaeser, D., Pickup, R., Pinay, G., Robertson, A. L., and Wood, P. J.: Inter-disciplinary perspectives on processes in the hyporheic zone, *Ecohydrology*, 4, 481–499, <https://doi.org/10.1002/eco.176>, 2011.
- Laan, M. M., Fulton, S. G., Garayburu-Caruso, V. A., Barnes, M. E., Borton, M. A., Chen, X., Farris, Y., Forbes, B., Goldman, A. E., Grieger, S., Hall Jr., R. O., Kaufman, M. H., Lin, X., Zionce, E. L. M., McKeever, S. A., Myers-Pigg, A., Otenburg, O., Pelly, A. C., Ren, H., Renteria, L., Scheibe, T. D., Son, K., Tagesstad, J., Torgeson, J. M., and Stegen, J. C.: Water column respiration in the Yakima River basin is explained by temperature, nutrients, and suspended solids, *Biogeosciences*, 22, 6137–6152, <https://doi.org/10.5194/bg-22-6137-2025>, 2025.
- Lewandowski, J., Arnon, S., Banks, E., Batelaan, O., Betterle, A., Broecker, T., Coll, C., Drummond, J. D., Gaona Garcia, J., Galloway, J., Gomez-Velez, J., Grabowski, R. C., Herzog, S. P., Hinkelmann, R., Höhne, A., Hollender, J., Horn, M. A., Jaeger, A., Krause, S., Löchner Prats, A., Magliozzi, C., Meinikmann, K., Mojarrad, B. B., Mueller, B. M., Peralta-Maraver, I., Popp, A. L., Posselt, M., Putschew, A., Radke, M., Raza, M., Riml, J., Robertson, A., Rutere, C., Schaper, J. L., Schirmer, M., Schulz, H., Shanafield, M., Singh, T., Ward, A. S., Wolke, P., Wörman, A., and Wu, L.: Is the Hyporheic Zone Relevant beyond the Scientific Community?, *Water*, 11, 2230, <https://doi.org/10.3390/w11112230>, 2019.
- Mancuso, J., Messick, E., and Tiegs, S. D.: Parsing spatial and temporal variation in stream ecosystem functioning, *Ecosphere*, 13, e4202, <https://doi.org/10.1002/ecs2.4202>, 2022.
- Mancuso, J., Tank, J. L., Mahl, U. H., Vincent, A., and Tiegs, S. D.: Monthly variation in organic-matter decomposition in agricultural stream and riparian ecosystems, *Aquat. Sci.*, 85, 83, <https://doi.org/10.1007/s00027-023-00975-7>, 2023.
- McClain, M. E., Boyer, E. W., Dent, C. L., Gergel, S. E., Grimm, N. B., Groffman, P. M., Hart, S. C., Harvey, J. W., Johnston, C. A., Mayorga, E., McDowell, W. H., and Pinay, G.: Biogeochemical Hot Spots and Hot Moments at the Interface of Terrestrial and Aquatic Ecosystems, *Ecosystems*, 6, 301–312, 2003.
- Mulholland, P. J., Fellows, C. S., Tank, J. L., Grimm, N. B., Webster, J. R., Hamilton, S. K., Martí, E., Ashkenas, L., Bowden, W. B., Dodds, W. K., McDowell, W. H., Paul, M. J., and Peterson, B. J.: Inter-biome comparison of factors controlling stream metabolism, *Freshwater Biol.*, 46, 1503–1517, <https://doi.org/10.1046/j.1365-2427.2001.00773.x>, 2001.
- Naegeli, M. W. and Uehlinger, U.: Contribution of the hyporheic zone to ecosystem metabolism in a prealpine gravel-bed-river, *J. N. Am. Benthol. Soc.*, 16, 794–804, 1997.
- Odum, H. T.: Primary production in flowing waters 1, *Limnol. Oceanogr.*, 1, 102–117, 1956.
- Piatka, D. R., Wild, R., Hartmann, J., Kaule, R., Kaule, L., Gilleföder, B., Peiffer, S., Geist, J., Beierkuhnlein, C., and Barth, J. A. C.: Transfer and transformations of oxygen in rivers as catchment reflectors of continental landscapes: A review, *Earth-Sci. Rev.*, 220, 103729, <https://doi.org/10.1016/j.earscirev.2021.103729>, 2021.
- Pingram, M. A., Clapcott, J. E., Hamer, M. P., Atalah, J., and Özkundakci, D.: Exploring temporal and spatial variation in cotton tensile-strength loss to assess the ecosystem health of non-wadeable rivers, *Ecol. Indic.*, 108, 105773, <https://doi.org/10.1016/j.ecolind.2019.105773>, 2020.
- Roley, S. S., Hall Jr., R. O., Perkins, W., Garayburu-Caruso, V. A., and Stegen, J. C.: Coupled primary production and respiration in a large river contrasts with smaller rivers and streams, *Limnol. Oceanogr.*, 68, 2461–2475, <https://doi.org/10.1002/lno.12435>, 2023.
- Rosemond, Amy D. et al.: Experimental nutrient additions accelerate terrestrial carbon loss from stream ecosystems, *Science*, 347, 1142–1145, <https://doi.org/10.1126/science.aaa1958>, 2015.
- Stegen, J. C., Barnes, M. E., Delgado, D., Forbes, B., Garayburu-Caruso, V. A., Goldman, A. E., Laan, M., McKeever, S. A., Regier, P., Renteria, L., and Tiegs, S. D.: Data and scripts associated with “Basin-scale connections between reach-scale sediment respiration and point-scale organic-matter decomposition”, River Corridor Hydro-biogeochemistry from Molecular to Multi-Basin Scales SFA, ESS-DIVE repository [data set], <https://doi.org/10.15485/3008446>, 2025.
- Talluto, L., del Campo, R., Estévez, E., Altermatt, F., Darty, T., and Singer, G.: Towards (better) fluvial meta-ecosystem ecology: a research perspective, *npj biodivers.*, 3, 1–10, <https://doi.org/10.1038/s44185-023-00036-0>, 2024.
- Tank, J. L., Rosi-Marshall, E. J., Griffiths, N. A., Entekin, S. A., and Stephen, M. L.: A review of allochthonous organic matter dynamics and metabolism in streams, *J. N. Am. Benthol. Soc.*, 29, 118–146, 2010.
- Tiegs, S. D., Clapcott, J. E., Griffiths, N. A., and Boulton, A. J.: A standardized cotton-strip assay for measuring organic-matter decomposition in streams, *Ecol. Indic.*, 32, 131–139, <https://doi.org/10.1016/j.ecolind.2013.03.013>, 2013.
- Tiegs, S. D., Costello, D. M., Isken, M. W., Woodward, G., McIntyre, P. B., Gessner, M. O., Chauvet, E., Griffiths, N. A., Flecker, A. S., Acuña, V., Albariño, R., Allen, D. C., Alonso, C., Andino, P., Arango, C., Aroviita, J., Barbosa, M. V. M., Barmuta, L. A., Baxter, C. V., Bell, T. D. C., Bellinger, B., Boyero, L., Brown, L. E., Bruder, A., Bruesewitz, D. A., Burdon, F. J., Callisto, M., Canhoto, C., Capps, K. A., Castillo, M. M., Clapcott, J., Colas, F., Colón-Gaud, C., Cornut, J., Crespo-Pérez, V., Cross, W. F., Culp, J. M., Danger, M., Dangles, O., Eyto, E. de, Derry, A. M., Villanueva, V. D., Douglas, M. M., Elozegi, A., Encalada, A. C., Entekin, S., Espinosa, R., Ethaiya, D., Ferreira, V., Ferriol, C., Flanagan, K. M., Fleituch, T., Shah, J. J. F., Frainer, A., Friberg, N., Frost, P. C., Garcia, E. A., Lago, L. G., Soto, P. E. G., Ghaté, S., Giling, D. P., Gilmer, A., Gonçalves, J. F., Gonzales, R. K., Graça, M. A. S., Grace, M., Grossart, H.-P., Guérol, F., Gulis, V., Hepp, L. U., Higgins, S., Hishi, T., Huddart, J., Hudson, J., Imberger, S., Iñiguez-Armijos, C., Iwata, T., Janetski, D. J., Jennings, E., Kirkwood, A. E., Koning, A. A., Kosten, S., Kuehn, K. A., Laudon, H., Leavitt, P. R., Silva, A. L. L. da, Leroux, S. J., LeRoy, C. J., Lisi, P. J., MacKenzie, R., Marcarelli, A. M., Masese, F. O., McKie, B. G., Medeiros, A. O., Meissner, K., Miliša, M., Mishra, S., Miyake, Y., Moerke, A., Mombrikotb, S., Mooney, R., Moulton, T., Muotka, T., Negishi, J. N., Neres-Lima, V., Nieminen, M. L., Nimptsch, J., Ondruch, J., Paavola, R., Pardo, I., Patrick, C. J., Peeters, E., Pozo, J., Pringle, C., Prussian, A., Quenta, E., Quesada, A., Reid, B., Richardson, J. S., Rigosi, A., Rincon, J., Risnoveanu, G., Robinson, C. T.,

- Rodriguez-Gallego, L., Royer, T. V., Rusak, J. A., Santamans, A. C., Selmecky, G. B., Simiyu, G., Skuja, A., Smykla, J., Sridhar, K. R., Sponseller, R., Stoler, A., Swan, C. M., Szlag, D., Teixeira-de Mello, F., Tonkin, J. D., Uusheimo, S., Veach, A. M., Vilbaste, S., Vought, L. B. M., Wang, C. P., Webster, J. R., Wilson, P. B., Woelfl, S., Xenopoulos, M. A., Yates, A. G., Yoshimura, C., Yule, C. M., Zhang, Y. X., and Zwart, J. A.: Global patterns and drivers of ecosystem functioning in rivers and riparian zones, *Science Advances*, 5, eaav0486, <https://doi.org/10.1126/sciadv.aav0486>, 2019.
- Tiegs, S. D., Capps, K. A., Costello, D. M., Schmidt, J. P., Patrick, C. J., Follstad Shah, J. J., Leroy, C. J., and CELLDIX Consortium†: Human activities shape global patterns of decomposition rates in rivers, *Science*, 384, 1191–1195, 2024.
- Vyšná, V., Dyer, F., Maher, W., and Norris, R.: Cotton-strip decomposition rate as a river condition indicator – Diel temperature range and deployment season and length also matter, *Ecol. Indic.*, 45, 508–521, <https://doi.org/10.1016/j.ecolind.2014.05.011>, 2014.
- Webb, J. R., Pearce, N. J. T., Painter, K. J., and Yates, A. G.: Hierarchical variation in cellulose decomposition in least-disturbed reference streams: a multi-season study using the cotton strip assay, *Landscape Ecol.*, 34, 2353–2369, <https://doi.org/10.1007/s10980-019-00893-w>, 2019.
- Wondzell, S. M.: The role of the hyporheic zone across stream networks, *Hydrol. Process.*, 25, 3525–3532, <https://doi.org/10.1002/hyp.8119>, 2011.
- Woodward, G., Gessner, M. O., Giller, P. S., Gulis, V., Hladyz, S., Lecerf, A., Malmqvist, B., McKie, B. G., Tiegs, S. D., and Cariss, H.: Continental-scale effects of nutrient pollution on stream ecosystem functioning, *Science*, 336, 1438–1440, 2012.
- Young, R. G. and Collier, K. J.: Contrasting responses to catchment modification among a range of functional and structural indicators of river ecosystem health, *Freshwater Biol.*, 54, 2155–2170, <https://doi.org/10.1111/j.1365-2427.2009.02239.x>, 2009.
- Young, R. G. and Huryn, A. D.: Effects of Land Use on Stream Metabolism and Organic Matter Turnover, *Ecol. Appl.*, 9, 1359–1376, [https://doi.org/10.1890/1051-0761\(1999\)009%5B1359:EOLUOS%5D2.0.CO;2](https://doi.org/10.1890/1051-0761(1999)009%5B1359:EOLUOS%5D2.0.CO;2), 1999.
- Zarnetske, J. P., Haggerty, R., Wondzell, S. M., and Baker, M. A.: Dynamics of nitrate production and removal as a function of residence time in the hyporheic zone, *J. Geophys. Res.-Biogeo.*, 116, <https://doi.org/10.1029/2010JG001356>, 2011.